Inorg. Chem. **2004**, *43*, 1751–1761

Synthesis and Characterization of Cu_2(I,I), Cu_2(I,II), and Cu_2(II,II) Compounds Supported by Two Phthalazine-Based Ligands: Influence of a Hydrophobic Pocket

Jane Kuzelka,[†] Sumitra Mukhopadhyay,[†] Bernhard Spingler,[‡] and Stephen J. Lippard*,[†]

Department of Chemistry, Massachusetts Institute of Technology, Cambridge, Massachusetts 02139, and Institute of Inorganic Chemistry, University of Zürich, CH-8057 Zürich, Switzerland

Received August 27, 2003

The copper coordination chemistry of two phthalazine-based ligands of differing steric bulk was investigated. A family of dinuclear complexes were prepared from reactions of $[Cu_2(bdptz)(MeCN)_2](OTf)_2$, **1**$(OTf)_2$, where bdptz = 1,4-bis(2,2′-dipyridylmethyl)phthalazine. Treatment of **1**$(OTf)_2$ with NaO_2CCH_3 afforded the class I mixed-valent compound $[Cu_2(bdptz)_2](OTf)_3$, **2**$(OTf)_3$, by disproportionation of Cu(I). Compound **2**$(OTf)_3$ displays an electron paramagnetic resonance spectrum, with $g_{\|} = 2.25$ ($A_{\|} = 169$ G) and $g_{\perp} = 2.06$, and exhibits a reversible redox wave at −452 mV versus Cp_2Fe^+/Cp_2Fe. The complex $[Cu_2(bdptz)(\mu\text{-}OH)(MeCN)_2](OTf)_3$, **3**$(OTf)_3$, was prepared by chemical oxidation of **1** with AgOTf, and exposure of **1** to dioxygen afforded $[Cu_2(bdptz)(\mu\text{-}OH)_2]_2(OTs)_4$, **4**$(OTs)_4$, which can also be obtained directly from $[Cu(H_2O)_6](OTs)_2$. In compound $[Cu_2(bdptz)(\mu\text{-}vpy)](OTf)_2$, **5**$(OTf)_2$, where vpy = 2-vinylpyridine, the vpy ligand bridges the two Cu(I) centers by using both its pyridine nitrogen and the olefin as donor functionalities. The sterically hindered compounds $[Cu_2(Ph_4bdptz)(MeCN)_2](OTf)_2$, **6**$(OTf)_2$, and $[Cu_2(Ph_4\text{-}bdptz)(\mu\text{-}O_2CCH_3)](OTf)$, **7**(OTf), were also synthesized, where Ph_4bdptz = 1,4-bis[bis(6-phenyl-2-pyridyl)methyl]-phthalazine. Complexes **1**–**7** were characterized structurally by X-ray crystallography. In **6** and **7**, the four phenyl rings form a hydrophobic pocket that houses the acetonitrile and acetate ligands. Complex **6** displays two reversible redox waves with $E_{1/2}$ values of +41 and +516 mV versus Cp_2Fe^+/Cp_2Fe. Analysis of oxygenated solutions of **6** by electrospray ionization mass spectrometry reveals probable aromatic hydroxylation of the Ph_4bdptz ligand. The different chemical and electrochemical behavior of **1** versus **6** highlights the influence of a hydrophobic binding pocket on the stability and reactivity of the dicopper(I) centers.

Introduction

The reductive activation of dioxygen by low-valent copper ions is accomplished in a variety of biological contexts. Numerous proteins employ copper to oxidize organic substrates,[1−5] bind dioxygen reversibly,[4,6] or mediate electron transfer.[4,7,8] The reduced forms of several copper metalloenzymes, notably hemocyanin,[4,6] tyrosinase,[4] and catechol oxidase,[3] feature active sites with coupled Cu(I) ions in a histidine-rich coordination environment. The copper centers interact with dioxygen to afford dicopper(II) peroxo species. This reaction is reversible for hemocyanin, whereas further activation of the peroxo unit occurs in both tyrosinase and catechol oxidase, ultimately resulting in aromatic ring oxidation.

Inspired by the natural systems, many laboratories have devoted significant effort to prepare small-molecule model compounds that mimic both the active site geometry and

* Author to whom correspondence should be addressed. E-mail: lippard@lippard.mit.edu.
† Massachusetts Institute of Technology.
‡ University of Zürich.

(1) Rogers, M. S.; Dooley, D. M. *Curr. Opin. Chem. Biol.* **2003**, *7*, 189−196.
(2) Lieberman, R. L.; Shrestha, D. B.; Doan, P. E.; Hoffman, B. M.; Stemmler, T. L.; Rosenzweig, A. C. *Proc. Natl. Acad. Sci. U.S.A.* **2003**, *100*, 3820−3825.
(3) Eicken, C.; Krebs, B.; Sacchettini, J. C. *Curr. Opin. Struct. Biol.* **1999**, *9*, 677−683.
(4) Solomon, E. I.; Sundaram, U. M.; Mackonkin, T. E. *Chem. Rev.* **1996**, *96*, 2563−2605.
(5) Klinman, J. P. *Chem. Rev.* **1996**, *96*, 2541−2561.
(6) Magnus, K. A.; Ton-That, H.; Carpenter, J. E. *Chem. Rev.* **1994**, *94*, 727−735.
(7) Messerschmidt, A. In *Multi-Copper Oxidases*; Messerschmidt, A., Ed.; World Scientific Publishing Co. Pte. Ltd.: Singapore, 1997; pp 23−79.
(8) Solomon, E. I.; Baldwin, M. J.; Lowery, M. D. *Chem. Rev.* **1992**, *92*, 521−542.

10.1021/ic035009r CCC: $27.50
Published on Web 02/04/2004

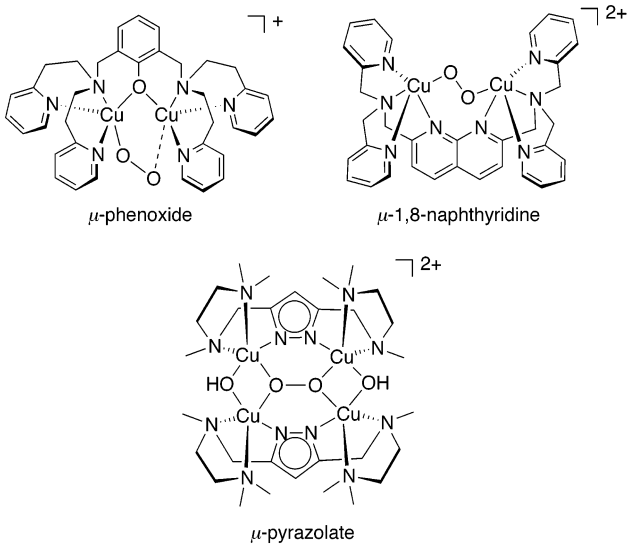

Figure 1. Examples of $\{Cu_2O_2\}$ adducts supported by multidentate dinucleating ligands.

dioxygen reactivity of these copper proteins.[9−14] Typically, mononuclear copper(I) complexes supported by various N-donor ligands or dicopper(I) compounds bearing ligands in which two clusters of nitrogen-rich moieties are linked by a hydrocarbon spacer react with dioxygen to afford Cu_2−O_2 adducts. There has been less work utilizing dinucleating ligands in which the linker moiety directly coordinates to and bridges two copper centers for the reductive activation of dioxygen. Several noteworthy examples are depicted in Figure 1, including a terminally bound peroxo species supported by a phenoxide bridge[15,16] and a relatively rigid 1,8-naphthyridine spacer that facilitates the formation of a (μ-1,2-peroxo) intermediate with a short copper···copper separation of ∼2.84 Å.[17] As a final example, a multidentate functionalized pyrazolate ligand allowed for the crystallographic characterization of an unusual tetranuclear (μ_4-peroxo)Cu_4(II) complex.[18] Clearly, dinucleating ligands enable the preparation of unique $\{Cu_2O_2\}$ species distinct from those generated by the reaction of dioxygen with mononuclear copper(I) complexes.

Although dramatic differences in the reactivity of mononuclear copper(I) compounds with dioxygen can result from small changes in the substituents of the ligand,[19] the effects of such perturbations in multidentate dinucleating ligands on the dioxygen reactivity of dicopper(I) complexes have not been as extensively investigated. We report here how such changes influence the chemistry of the phthalazine-supported dicopper compounds. Previously, we employed the nitrogen-rich hexadentate ligands bdptz and Ph_4bdptz (Chart 1), where bdptz is 1,4-bis(2,2′-dipyridylmethyl)-phthalazine and Ph_4bdptz is 1,4-bis[bis(6-phenyl-2-pyridyl)-methyl]phthalazine, to prepare dinuclear compounds of several divalent first-row transition-metal ions.[20−24] These two dinucleating ligands feature a phthalazine bridge linking two clusters of pyridine groups and support dimetallic structures with a variety of ancillary ligands. In this paper, we describe the copper(I) and copper(II) chemistry of these two phthalazine-based ligands. The readily assembled complex $[Cu_2(bdptz)(MeCN)_2](OTf)_2$, **1**$(OTf)_2$, serves as a convenient starting material for preparing the compounds $[Cu_2(bdptz)_2](OTf)_3$, **2**$(OTf)_3$, $[Cu_2(bdptz)(\mu\text{-}OH)(MeCN)_2]$-$(OTf)_3$, **3**$(OTf)_3$, $[Cu_2(bdptz)(\mu\text{-}OH)_2]_2(OTs)_4$, **4**$(OTs)_4$, and $[Cu_2(bdptz)(\mu\text{-}vpy)](OTf)_2$, **5**$(OTf)_2$.[25] The use of Ph_4bdptz permitted the isolation of $[Cu_2(Ph_4bdptz)(MeCN)_2](OTf)_2$, **6**$(OTf)_2$, and $[Cu_2(Ph_4bdptz)(\mu\text{-}O_2CCH_3)](OTf)$, **7**(OTf). All of the compounds were studied by X-ray crystallography, and the electrochemical behavior of **1**, **2**, and **6** was investigated. Pronounced differences in the reactivity and stability between the two series of complexes derived from bdptz and Ph_4bdptz were encountered. Our results show that the attachment of a hydrophobic binding pocket to a multidentate ligand platform, a feature highly desirable for facilitating the activation of small-molecule substrates, dramatically influences the properties of the resulting

Chart 1

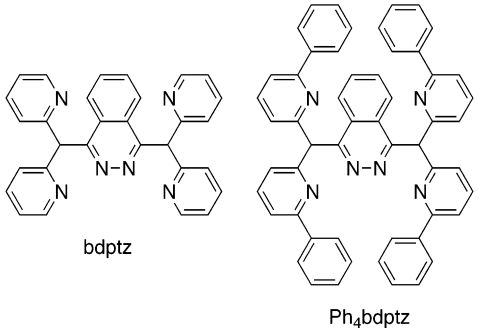

(9) Zhang, C. X.; Liang, H.-C.; Humphreys, K. J.; Karlin, K. D. In *Catalysis by Metal Complexes*; James, B. R., van Leeuwen, P. W. N. M., Eds.; Kluwer Academic Publishers: Dordrecht, The Netherlands, 2003; Vol. 26, pp 79−121.
(10) Stack, T. D. P. *Dalton Trans.* **2003**, 1881−1889.
(11) Itoh, S.; Fukuzumi, S. *Bull. Chem. Soc. Jpn.* **2002**, *75*, 2081−2095.
(12) Schindler, S. *Eur. J. Inorg. Chem.* **2000**, 2311−2326.
(13) Tolman, W. B. *Acc. Chem. Res.* **1997**, *30*, 227−237.
(14) Kitajima, N.; Moro-oka, Y. *Chem. Rev.* **1994**, *94*, 737−757.
(15) Pate, J. E.; Cruse, R. W.; Karlin, K. D.; Solomon, E. I. *J. Am. Chem. Soc.* **1987**, *109*, 2624−2630.
(16) Karlin, K. D.; Cruse, R. W.; Gultneh, Y.; Hayes, J. C.; Zubieta, J. *J. Am. Chem. Soc.* **1984**, *106*, 3372−3374.
(17) He, C.; DuBois, J. L.; Hedman, B.; Hodgson, K. O.; Lippard, S. J. *Angew. Chem., Int. Ed.* **2001**, *40*, 1484−1487.
(18) Meyer, F.; Pritzkow, H. *Angew. Chem., Int. Ed.* **2000**, *39*, 2112−2115.
(19) Liang, H.-C.; Zhang, C. X.; Henson, M. J.; Sommer, R. D.; Hatwell, K. R.; Kaderli, S.; Zuberbühler, A. D.; Rheingold, A. L.; Solomon, E. I.; Karlin, K. D. *J. Am. Chem. Soc.* **2002**, *124*, 4170−4171.
(20) Kuzelka, J.; Spingler, B.; Lippard, S. J. *Inorg. Chim. Acta* **2002**, *337*, 212−222.
(21) Barrios, A. M.; Lippard, S. J. *Inorg. Chem.* **2001**, *40*, 1060−1064.
(22) Barrios, A. M.; Lippard, S. J. *Inorg. Chem.* **2001**, *40*, 1250−1255.
(23) Barrios, A. M.; Lippard, S. J. *J. Am. Chem. Soc.* **2000**, *122*, 9172−9177.
(24) Barrios, A. M.; Lippard, S. J. *J. Am. Chem. Soc.* **1999**, *121*, 11751−11757.
(25) Abbreviations used: OTf^- = triflate; OTs^- = tosylate; vpy = 2-vinylpyridine; bdpdz = 3,6-bis(di-2-pyridylmethyl)pyridazine; TMPA = tris(2-pyridylmethyl)amine; H-MePY2 = bis[2-(2-pyridyl)ethyl]-methylamine; bTMPA = 6,6′-bis[[bis(2-pyridylmethyl)amino]methyl]-2,2′-bipyridine; L^0 = tris(2-pyridyl)methoxymethane; L^2 = 5,5,16,16-tetramethyl-23,24-dioxa-3,7,14,18-tetraazatricyclo[18.2.1.1^{9,12}]tetracosa-1(22),2,7,9,11,13,18,20-octaene; D^1 = [5-(2-{6-[(bis(2-pyridylmethylamino))methyl]-3-pyridyl}ethyl)−(2-pyridylmethyl)]bis(2-pyridylmethyl)amine; BBAN = 2,7-bis(*N*,*N*-dibenzylaminomethyl)-1,8-naphthyridine; $[BAr'_4]^-$ = $[(3,5\text{-}(CF_3)_2C_6H_3)_4B]^-$.

coordination compounds relative to the complexes lacking such a binding cavity.

Experimental Section

General Procedures. Dichloromethane, acetonitrile, and diethyl ether were saturated with argon and purified by passage over a column of activated alumina under argon.[26] Methanol was distilled from Mg and I_2 under nitrogen. The compounds $[Cu(MeCN)_4]X$ (X = OTf[27] or BF_4[28]), bdptz,[24] and Ph_4bdptz[20] were prepared according to published literature procedures. Prior to use, vpy was freshly distilled. All other reagents were purchased from commercial sources and used as received. Air-sensitive manipulations, including the synthesis of the triflate salts of **1**−**3** and **5**−**7**, were performed under nitrogen in an MBraun glovebox or by using standard Schlenk techniques.

$[Cu_2(bdptz)(MeCN)_2](OTf)_2$, 1(OTf)$_2$. To a colorless solution of $[Cu(MeCN)_4](OTf)$ (404 mg, 1.07 mmol) in MeCN (5 mL) was added solid bdptz (253 mg, 0.543 mmol) to generate an orange suspension. After further addition of MeCN (∼4 mL), the solution became homogeneous and was stirred for 30 min. The orange solution was saturated with Et_2O and left at room temperature overnight to give **1**$(OTf)_2$ as an orange microcrystalline solid (436 mg, 83%). FTIR (cm^{-1}, KBr): 3126 (w), 3097 (w), 3073 (w), 3051 (w), 3000 (w), 2932 (w), 1596 (s), 1569 (m), 1536 (w), 1473 (m), 1441 (s), 1414 (w), 1364 (m), 1328 (w), 1300 (s), 1284 (s), 1261 (s), 1238 (s), 1165 (m), 1147 (m), 1029 (s), 861 (w), 822 (w), 771 (s), 759 (s), 683 (w), 637 (s), 573 (s), 517 (m). ^{1}H NMR (300 MHz, CD_2Cl_2) δ: 9.16 m (2H), 8.69 d (J = 13 Hz, 4H), 8.27 m (2H), 8.11 d (J = 26 Hz, 4H), 7.81 m (4H), 7.36 m (4H), 7.08 s (2H), 2.47 s (6H). Anal. Calcd for $C_{36}H_{28}N_8O_6F_6S_2Cu_2$: C, 44.40; H, 2.90; N, 11.51. Found: C, 44.16; H, 2.86; N, 11.38.

$[Cu_2(bdptz)_2](OTf)_3$, 2(OTf)$_3$. To an orange solution of **1**$(OTf)_2$ (50 mg, 0.051 mmol) in MeOH (2 mL) was added dropwise a solution of NaO_2CCH_3 (8.4 mg, 0.10 mmol) in MeOH (2 mL). A red-brown mixture was generated and stirred for 2 h. Filtration through a plug of Celite followed by exposure to Et_2O vapor diffusion yielded **2**$(OTf)_3$ as a red crystalline solid (20 mg, 53%). Single crystals of **2**$(OTf)_3$·2MeCN·0.5Et_2O suitable for X-ray diffraction study were grown from MeCN by Et_2O vapor diffusion. FTIR (cm^{-1}, KBr): 3062 (w), 3022 (w), 2929 (w), 1596 (m), 1596 (m), 1570 (m), 1546 (w), 1472 (m), 1442 (m), 1405 (m), 1364 (m), 1276 (s), 1223 (m), 1150 (m), 1054 (w), 1030 (s), 854 (w), 832 (w), 817 (w), 759 (m), 685 (w), 680 (w), 655 (w), 636 (s), 585 (m), 572 (m), 517 (m). Anal. Calcd for $C_{63}H_{44}N_{12}O_9F_9S_3Cu_2$: C, 50.20; H, 2.94; N, 11.15. Found: C, 49.91; H, 2.77; N, 11.19.

$[Cu_2(bdptz)(\mu\text{-}OH)(MeCN)_2](OTf)_3$, 3(OTf)$_3$. To an orange solution of **1**$(OTf)_2$ (100 mg, 0.103 mmol) in MeOH (4 mL) was added AgOTf (53 mg, 0.21 mmol) in MeOH (2 mL), and a cloudy, yellow-green mixture was formed. The suspension was stirred for 30 min, followed by filtration through Celite and evaporation of the solvent under reduced pressure. Blue X-ray quality crystals of **3**$(OTf)_3$·1.75MeCN were obtained by vapor diffusion of Et_2O into a solution of MeCN and CH_2Cl_2 (47 mg, 40%). FTIR (cm^{-1}, KBr): 3219 (br, m), 1670 (w), 1611 (m), 1575 (w), 1479 (w), 1450 (m), 1373 (w), 1289 (s), 1237 (s), 1165 (s), 1029 (s), 823 (w), 772 (m), 685 (w), 637 (s), 578 (m), 517 (m). Difficulty in separating **3**$(OTf)_3$ from an oil that formed upon crystallization prevented satisfactory elemental combustion analysis.

$[Cu_2(bdptz)(\mu\text{-}OH)_2]_2(OTs)_4$, 4(OTs)$_4$. Method A. A solution of $[Cu(H_2O)_6](OTs)_2$ (110 mg, 0.215 mmol) in MeCN/H_2O (10:1, 4 mL) was treated with solid bdptz (50 mg, 0.11 mmol) to generate a dark-blue solution to which an aqueous solution of NaOH (1 M, 215 μL, 0.215 mmol) was added. The resulting blue-green mixture was stirred for 30 min and filtered through Celite, and Et_2O vapor was allowed to diffuse into the solution. Green crystals of **4**$(OTs)_4$·MeCN·12H_2O, suitable for X-ray diffraction study, were isolated (30 mg, 29%). FTIR (cm^{-1}, KBr): 3447 (br, m), 3076 (w), 3048 (w), 3008 (w), 2919 (w), 2868 (w), 1607 (m), 1592 (m), 1570 (w), 1473 (w), 1444 (m), 1364 (w), 1233 (m), 1212 (s), 1191 (s), 1165 (s), 1118 (s), 1031 (s), 1008 (s), 918 (w), 875 (w), 819 (m), 769 (m), 680 (s), 650 (w), 636 (w), 625 (w), 581 (w), 563 (s), 549 (m), 526 (w). Anal. Calcd for $C_{88}H_{78}N_{12}O_{17}S_4Cu_4$, **4**$(OTs)_4$·$H_2O$: C, 53.98; H, 4.02; N, 8.58. Found: C, 53.76; H, 3.81; N, 8.61.

Method B. An orange solution of **1**$(OTf)_2$ (65 mg, 0.067 mmol) in MeCN (4 mL) was gently purged with O_2 for 45 min to yield a green solution. An aqueous solution of NaOTs (2.7 M, 0.5 mL, 1.3 mmol) was added dropwise to afford a green precipitate, which was collected on filter paper and washed with H_2O. Slow evaporation of the filtrate gave green crystals of **4**$(OTs)_4$ (30 mg, 46%).

$[Cu_2(bdptz)(\mu\text{-}vpy)](OTf)_2$, 5(OTf)$_2$. Treatment of **1**$(OTf)_2$ (150 mg, 0.154 mmol) with vpy (18.3 μL, 0.170 mmol) in CH_2Cl_2 (6 mL) afforded a yellow mixture, which was stirred for 30 min. Filtration through Celite was followed by evaporation of the solvent under reduced pressure. The resulting residue was dissolved in MeOH, and Et_2O vapor was allowed to diffuse into the solution. Orange crystals of **5**$(OTf)_2$·Et_2O, suitable for X-ray crystallography, were obtained by this procedure (128 mg, 86%). FTIR (cm^{-1}, KBr): 3131 (w), 3073 (w), 2976 (w), 2933 (w), 2855 (w), 1598 (s), 1570 (m), 1549 (w), 1531 (w), 1473 (m), 1442 (m), 1419 (w), 1365 (w), 1351 (w), 1260 (s), 1223 (m), 1161 (m), 1115 (w), 1029 (s), 937 (w), 861 (w), 774 (m), 756 (m), 679 (w), 637 (s), 585 (m), 572 (m), 517 (m). ^{1}H NMR (300 MHz, CD_2Cl_2) δ: 9.39 m (1H), 9.27 m (1H), 8.89 d (J = 18 Hz, 1H), 8.72 dd (J = 14 Hz, 2H), 8.56 d (J = 14 Hz, 1H), 8.37 d (J = 18 Hz, 2H), 8.29−8.10 m (7H), 7.92−7.82 m (3H), 7.71 m (1H), 7.57 m (1H), 7.48−7.34 m (5H), 7.24−7.13 m (2H), 5.60 d (J = 53 Hz, 1H), 4.85 d (J = 31 Hz, 1H). Anal. Calcd for $C_{39}H_{29}N_7O_6F_6S_2Cu_2$: C, 46.99; H, 2.93; N, 9.84. Found: C, 47.19; H, 3.17; N, 9.99.

$[Cu_2(Ph_4bdptz)(MeCN)_2](OTf)_2$, 6(OTf)$_2$. To a solution of $[Cu(MeCN)_4](OTf)$ (67 mg, 0.18 mmol) in MeCN (10 mL) was added solid Ph_4bdptz (69 mg, 0.090 mmol), and the resulting orange mixture was stirred for 30 min. The slightly cloudy solution was filtered through Celite and evaporated to dryness. The residue was dissolved in CH_2Cl_2, and Et_2O vapor diffusion into this solution afforded **6**$(OTf)_2$ as a yellow flocculent solid (83 mg, 73%). X-ray quality crystals of the BF_4^- salt, **6**$(BF_4)_2$, were obtained from the corresponding reaction using $[Cu(MeCN)_4](BF_4)$, followed by recrystallization from MeCN with Et_2O vapor diffusion. FTIR (cm^{-1}, KBr): 3062 (w), 3033 (w), 2993 (w), 2932 (w), 1591 (s), 1579 (m), 1561 (s), 1542 (m), 1497 (w), 1448 (s), 1421 (m), 1357 (m), 1263 (s), 1223 (s), 1148 (s), 1030 (s), 919 (w), 813 (m), 764 (s), 699 (s), 676 (m), 637 (s), 572 (m), 516 (m). ^{1}H NMR (300 MHz, CH_2Cl_2) δ: 9.36 m (2H), 8.37 m (2H), 8.20 d (J = 25 Hz, 4H), 7.92 t (J = 25 Hz, 4H), 7.55−7.45 m (16H), 7.40−7.32 m (10H), 1.21 s (6H). Anal. Calcd for $C_{60}H_{44}N_8O_6F_6S_2Cu_2$: C, 56.38; H, 3.47; N, 8.77. Found: C, 56.09; H, 3.38; N, 8.67.

$[Cu_2(Ph_4bdptz)(\mu\text{-}O_2CCH_3)](OTf)$, 7(OTf). To a mixture of **6**$(OTf)_2$ (52 mg, 0.041 mmol) in CH_2Cl_2 (4 mL) was added dropwise a solution of NaO_2CCH_3 (6.7 mg, 0.081 mmol) in MeOH (1 mL). The resulting dark-red solution was stirred for 30 min and evaporated to dryness under reduced pressure. The residue was

(26) Pangborn, A. B.; Giardello, M. A.; Grubbs, R. H.; Rosen, R. K.; Timmers, F. J. *Organometallics* **1996**, *15*, 1518−1520.
(27) Kubas, G. J. In *Inorganic Synthesis*; Shriver, D. F., Ed.; John Wiley & Sons: New York, 1979; Vol. 19, pp 90−92.
(28) Heckel, E. *Chem. Abstr.* **1967**, *66*, 46487e.

dissolved in CH_2Cl_2 and filtered through Celite, and diffusion of Et_2O vapor into this solution afforded a mixture of **6**$(OTf)_2$ and **7**(OTf), as revealed by an X-ray diffraction study. FTIR (cm^{-1}, KBr): 3062 (w), 3032 (w), 2923 (w), 1589 (s), 1579 (s), 1559 (s), 1448 (s), 1420 (m), 1358 (w), 1280 (s), 1255 (s), 1223 (w), 1156 (m), 1029 (s), 821 (w), 808 (m), 782 (w), 760 (s), 742 (w), 697 (s), 693 (s), 653 (w), 638 (s), 573 (w), 517 (w).

Physical Measurements. ^{1}H NMR spectra were obtained on a 300 MHz Varian Mercury spectrometer. FTIR spectra were recorded on a Thermo Nicolet Avatar 360 spectrometer. Optical spectra were measured on a Hewlett-Packard 8453 diode-array spectrophotometer, and low-temperature experiments were carried out by using a custom-made quartz cuvette fused onto a vacuum-jacketed Dewar. Frozen solution electron paramagnetic resonance (EPR) spectra of **2**$(OTf)_3$ were recorded on a Bruker model 300 electron spin polarization (ESP) X-band spectrometer operating at 9.37 GHz and running WinEPR software. A temperature of 77 K was maintained by using a specially designed coldfinger filled with liquid N_2. Electrospray ionization mass spectrometry (ESI-MS) spectra of oxidized solutions of **6**$(OTf)_2$ were obtained on a Bruker Daltonics APEXII Tesla Fourier transform mass spectrometer in the MIT Department of Chemistry Instrumentation Facility (Figures S1−S3 in the Supporting Information).

Collection and Reduction of X-ray Data. Single crystals were coated in Infineum V8512 oil (formerly called Paratone N oil) on the ends of glass capillaries (0.1 mm diameter) and rapidly cooled under a low-temperature nitrogen cold stream maintained by a Bruker KRYOFLEX BVT-AXS nitrogen cryostat. Crystals of **6**$(BF_4)_2$ were found to be thermally sensitive, and room temperature data for this structure were subsequently acquired. Intensity data were collected on a Bruker SMART (**1**−**3**) or APEX (**4**−**7**) CCD (charge-coupled device) X-ray diffractometer with graphite-monochromatized Mo Kα radiation (λ = 0.710 73 Å), controlled by a Pentium-based PC running the SMART software package.[29] Crystals were mounted on a three-circle goniometer with χ fixed at 54.73°, and the diffracted radiation was detected on a phosphor screen that was maintained at 0 °C and held at a fixed distance of 6.0 cm from the crystal. Least-squares analysis of the unit-cell parameters of a well-centered ylide test crystal was used to determine the detector center and the crystal-to-detector distance. A preliminary unit cell of a carefully optically centered crystal was calculated by a series of 20 or 30 data frames, measured at 0.3° increments of ω, with three different 2θ and ϕ values. A total of 16 frames were collected with exposure times of 10 or 30 s in the absence of the X-ray beam to correct for the background detector current. The detector was positioned at a 2θ value of 29.10°, and data were measured using ω scans of 0.3° per frame with either 10 or 30 s exposure, such that a hemisphere of 25−28.29° was collected. A series of 600 frames were collected in each of the first three shells, and the initial 50 frames of the first shell were re-collected at the end of the data collection in order to check for any crystal decay. The starting positions of the crystal for the first three shells were $\phi = 0°$ and $\omega = -28°$, $\phi = 90°$ and $\omega = -28°$, and $\phi = 180°$ and $\omega = -28°$, respectively. The raw data frames were integrated using the SAINT software,[30] and the orientation matrix, initial background, and spot shape measurements were continuously updated during the integration. Background frame information was updated as indicated in eq 1, where B' is the update

$$B' = (7B + C)/8 \quad (1)$$

pixel value, B is the background pixel value prior to updating, and C is the pixel value of the current frame. Spatial distortions induced by the detector and pixels residing outside the active area of the detector or behind the beam stop were masked during the integration.

The structures were solved by direct methods using SHELXS-97 software[31] and refined on F^2 by using the SHELXL-97 program[32] incorporated in the SHELXTL[33] software package. Empirical absorption corrections were applied by using the SADABS program,[34] and PLATON software[35] was used to check the possibility of higher symmetry. All non-hydrogen atoms were located, and their positions were refined with anisotropic thermal parameters by least-squares cycles and Fourier syntheses. Hydrogen atoms were assigned idealized positions and given a thermal parameter 1.2 times the thermal parameter of the carbon atom to which each was attached.

The Et_2O molecule in the structure of **2** is located on a special position and has disordered methylene carbon atoms, each of which was modeled at 50% occupancy. In the structure of **3**, one triflate is disordered over two positions and was refined with occupancies of 58 and 42%. Four acetonitrile solvent molecules are present in the lattice. One of these molecules is located on a special position and was refined with 50% occupancy; a second molecule was also modeled with 50% occupancy, and the remaining two solvent molecules share a common methyl group and were refined with occupancies of 50 and 25%, with the occupancy of the shared carbon atom being 75%. The structure of **4** includes 2 acetonitrile solvent molecules that were refined with 50% occupancy and 18 water molecules, 8 of which were modeled with full occupancy, 6 with 50% occupancy, and 4 with 25% occupancy. In the structure of **5**, the oxygen atom of the Et_2O solvent molecule was refined over two positions with occupancies of 75 and 25%. One fluorine atom of a tetrafluoroborate counterion in the structure of **6**$(BF_4)_2$ is disordered over two positions and was modeled with occupancies of 50%. Crystallographic data for compounds **2**−**6** are listed in Table 1, and selected bond lengths and angles of the compounds are listed in Tables 2−4. Complete atom-labeling schemes are provided in Figures S4−S8 in the Supporting Information.

Electrochemistry. Cyclic voltammograms were recorded in an MBraun glovebox under a nitrogen atmosphere using an EG&G model 263 potentiostat. The three-component cell consisted of a platinum working electrode, $Ag/AgNO_3$ (0.1 M in MeCN) reference electrode, and platinum wire auxiliary electrode. The supporting electrolyte was a 0.5 M $Bu_4N(PF_6)$ solution. All of the measurements were referenced externally to Cp_2Fe. Linear plots of current versus (scan rate)$^{1/2}$ for **2**$(OTf)_3$ and **6**$(OTf)_2$ are displayed in Figures S9 and S10 in the Supporting Information, respectively.

Results and Discussion

Synthesis of a Dicopper(I) Starting Material. Compound **1**$(OTf)_2$ was obtained in good yield (>80%) by the reaction of $[Cu(MeCN)_4](OTf)$ and bdptz in a 2:1 ratio. Although

(29) *SMART: Software for the CCD Detector System*, version 5.626; Bruker AXS: Madison, WI, 2000.
(30) *SAINT: Software for the CCD Detector System*, version 5.01; Bruker AXS: Madison, WI, 1998.
(31) Sheldrick, G. M. *SHELXS-97: Program for the Solution of Crystal Structure*; University of Göttingen: Göttingen, Germany, 1997.
(32) Sheldrick, G. M. *SHELXL-97: Program for the Solution of Crystal Structure*; University of Göttingen: Göttingen, Germany, 1997.
(33) *SHELXTL: Program Library for Structure Solution and Molecular Graphics*, version 5.10; Bruker AXS: Madison, WI, 1998.
(34) Sheldrick, G. M. *SADABS: Area-Detector Absorption Correction*; University of Göttingen: Göttingen, Germany, 1996.
(35) Spek, A. L. *PLATON, A Multipurpose Crystallographic Tool*; Utrecht University: Utrecht, The Netherlands, 2000.

Table 1. Summary of X-ray Crystallographic Data

	2$(OTf)_3$·2MeCN·0.5Et_2O	**3**$(OTf)_3$·1.75MeCN	**4**$(OTs)_4$·MeCN·12H_2O	**5**$(OTf)_2$·Et_2O	**6**$(BF_4)_2$
formula	$C_{69}H_{44}N_{14}Cu_2O_{9.5}S_3F_9$	$C_{40.5}H_{23}N_{9.75}Cu_2O_{10}S_3F_9$	$C_{90}H_{79}N_{13}Cu_4O_{28}S_4$	$C_{43}H_{29}N_7Cu_2O_7S_2F_6$	$C_{58}H_{38}N_8Cu_2B_2F_8$
fw	1615.44	1200.45	2173.06	1060.93	1147.66
space group	$P\bar{1}$	$C2/c$	$P2_1/c$	$P2_1/n$	$P\bar{1}$
a (Å)	15.408(5)	21.197(4)	14.128(2)	15.005(8)	11.355(2)
b (Å)	15.733(5)	23.198(4)	25.037(4)	18.358(10)	14.373(3)
c (Å)	15.804(5)	22.497(4)	14.146(2)	16.459(9)	17.592(3)
α (deg)	67.990(5)				85.391(4)
β (deg)	77.430(5)	111.357(3)	95.695(3)	91.162(8)	80.904(3)
γ (deg)	83.600(5)				66.756(3)
V (Å^3)	3464.9(19)	10 303(3)	4979.3(13)	4533(4)	2604.4(9)
Z	2	8	2	4	2
T (°C)	−85	−85	−70	−100	22
ρ_{calcd} (g cm^{-3})	1.548	1.548	1.449	1.555	1.463
μ(Mo Kα) (mm^{-1})	0.798	1.042	1.008	1.113	0.893
θ range (deg)	1.42−25.00	1.35−25.00	1.63−28.26	1.66−28.29	1.17−25.00
total no. of data	18 335	26 967	30 356	27 923	13 599
no. of unique data	12 069	9099	11 380	10 330	8491
observed data[a]	9471	5664	8774	8497	7127
no. of parameters	970	683	658	613	712
R1[a,b]	0.0413	0.0761	0.0492	0.0500	0.0602
wR2[a,c]	0.1011	0.2162	0.1281	0.1226	0.1594
max, min peaks (e Å^{-3})	0.653, −0.457	1.054, −0.887	0.788, −0.410	0.749, −0.337	1.187, −0.407

[a] Observation criterion: $I > 2\sigma(I)$. [b] $R1 = \sum||F_o| - |F_c||/\sum|F_o|$. [c] $wR2 = \{\sum[w(F_o^2 - F_c^2)^2]/\sum[w(F_o^2)^2]\}^{1/2}$.

Table 2. Selected Bond Lengths (Å) and Angles (deg) for **2** and **3**[a]

	bond lengths		bond angles	
2	Cu1···Cu2	5.2037(15)	N1−Cu1−N4	85.35(10)
	Cu1−N1	2.036(3)	N1−Cu1−N7	93.93(10)
	Cu1−N3	2.035(3)	N4−Cu1−N10	178.43(10)
	Cu1−N4	2.287(3)	N7−Cu1−N10	86.84(10)
	Cu1−N7	2.030(2)	N3−Cu1−N9	94.96(10)
	Cu1−N9	2.065(3)	N5−Cu2−N6	90.77(10)
	Cu1−N10	2.299(3)	N5−Cu2−N11	119.09(10)
	Cu2−N5	2.076(3)	N5−Cu2−N12	110.31(10)
	Cu2−N6	2.035(3)	N6−Cu2−N12	142.69(10)
	Cu2−N11	2.090(3)		
	Cu2−N12	2.020(2)		
3	Cu1···Cu2	3.1774(12)	Cu1−O1−Cu2	112.8(3)
	Cu1−N1	2.048(6)	N1−Cu1−N3	86.7(2)
	Cu1−N3	2.299(6)	N1−Cu1−N4	88.1(2)
	Cu1−N4	2.006(6)	N3−Cu1−N4	82.7(2)
	Cu1−N7	1.993(8)	O1−Cu1−N3	105.66(19)
	Cu1−O1	1.909(5)	O1−Cu1−N4	168.6(2)
	Cu2−N2	2.046(6)	N2−Cu2−N5	84.9(2)
	Cu2−N5	2.264(6)	N2−Cu2−N6	87.8(2)
	Cu2−N6	2.001(6)	N5−Cu2−N6	85.4(2)
	Cu2−N8	2.006(8)	O1−Cu2−N5	100.7(2)
	Cu2−O1	1.905(5)	O1−Cu2−N6	169.8(2)

[a] Numbers in parentheses are the estimated standard deviations of the last significant figure. Atoms are labeled as indicated in Figure 2.

Table 3. Selected Bond Lengths (Å) and Angles (deg) for **4** and **5**[a]

	bond lengths		bond angles	
4	Cu1···Cu2	3.1690(7)	Cu1−O1−Cu2	112.47(10)
	Cu1···Cu2A	3.5603(7)	Cu2−O2−Cu1A	135.19(12)
	Cu1−N1	2.053(2)	N1−Cu1−N3	81.67(9)
	Cu1−N3	2.275(3)	N1−Cu1−N4	86.83(10)
	Cu1−N4	2.021(2)	N3−Cu1−N4	88.16(10)
	Cu1−O1	1.905(2)	O1−Cu1−N3	98.50(9)
	Cu1−O2A	1.926(2)	O1−Cu1−N4	168.70(10)
	Cu2−N2	2.066(2)	N2−Cu2−N5	81.53(9)
	Cu2−N5	2.327(3)	N2−Cu2−N6	87.43(10)
	Cu2−N6	2.016(3)	N5−Cu2−N6	84.88(10)
	Cu2−O1	1.907(2)	O1−Cu2−N5	100.28(10)
	Cu2−O2	1.925(2)	O1−Cu2−N6	170.08(9)
5	Cu1···Cu2	3.7024(13)	N1−Cu1−N3	87.69(9)
	Cu1−N1	2.144(2)	N1−Cu1−N4	88.60(9)
	Cu1−N3	2.144(2)	N3−Cu1−N4	91.64(10)
	Cu1−N4	2.015(2)	N1−Cu1−N7	124.40(9)
	Cu1−N7	1.951(2)	N3−Cu1−N7	115.08(10)
	Cu2−N2	2.018(2)	N4−Cu1−N7	136.24(10)
	Cu2−N5	2.103(3)	N2−Cu2−N5	89.54(9)
	Cu2−N6	2.060(2)	N2−Cu2−N6	90.90(9)
	Cu2−C36	2.050(3)	N5−Cu2−N6	89.84(10)
	Cu2−C37	2.008(3)		
	C36−C37	1.368(4)		

[a] Numbers in parentheses are the estimated standard deviations of the last significant figure. Atoms are labeled as indicated in Figure 2.

the ability of bdptz to promote the formation of dinuclear complexes is well established,[21−24] **1** is the first example of a dicopper(I) compound with this ligand. X-ray crystallographic analysis was sufficient to ascertain the structure of **1**, but poor data quality precluded a satisfactory refinement, and substitution of the triflate counterions for other units did not afford better crystals. The cationic moiety contains two Cu(I) centers, ∼3.74 Å apart, bridged by the phthalazine unit and further ligated by the pyridine rings of bdptz and two MeCN solvent molecules. NMR spectroscopy and elemental analysis support the formulation of compound **1**$(OTf)_2$. Coordination of acetonitrile rather than the triflate counterions to the metal centers reflects its good solvation properties, and the ability to substitute these coordinated solvent molecules for other ligands renders **1** a convenient starting material for preparing a variety of compounds, as shown in Scheme 1.

Preparation and Characterization of a Mixed-Valent Cu(I)Cu(II) Compound. Treatment of **1**$(OTf)_2$ with NaO_2CCH_3 in MeOH did not yield the anticipated acetate-bridged complex. Rather, the mixed-valent Cu(I)Cu(II) compound **2**$(OTf)_3$ was isolated. The concomitant precipitation of Cu metal over the course of the reaction suggests that disproportionation of Cu(I) is responsible for the generation of the divalent metal component.[36] Initial coordination of the acetate to copper(I) probably occurs, followed by disproportionation and rearrangement to afford **2**.

Scheme 1

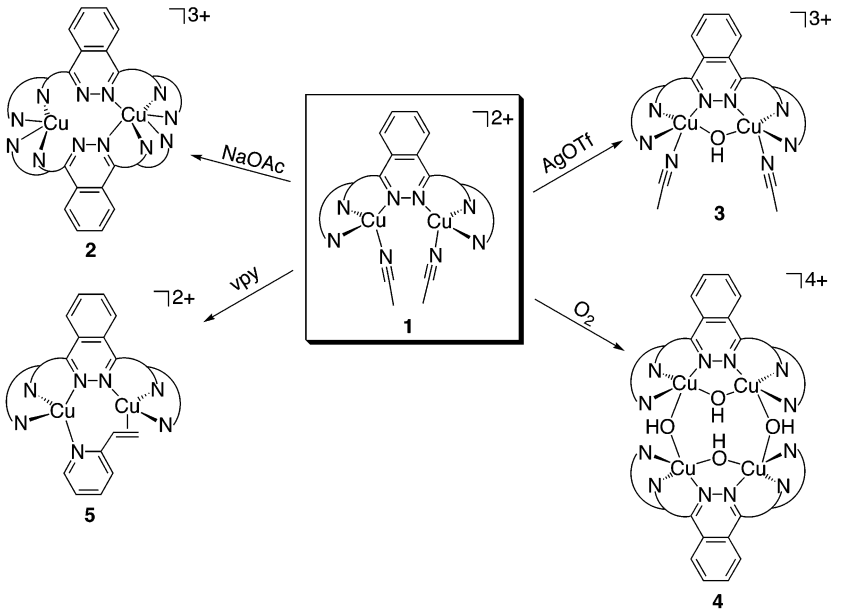

Table 4. Selected Bond Lengths (Å) and Angles (deg) for **6**[a]

	bond lengths		bond angles	
6	Cu1···Cu2	3.7923(9)	N1−Cu1−N3	91.64(15)
	Cu1−N1	2.141(4)	N1−Cu1−N4	88.23(14)
	Cu1−N3	2.132(4)	N1−Cu1−N7	120.23(15)
	Cu1−N4	2.069(4)	N3−Cu1−N4	90.36(15)
	Cu1−N7	1.893(4)	N2−Cu2−N5	90.32(15)
	Cu2−N2	2.099(4)	N2−Cu2−N6	89.54(14)
	Cu2−N5	2.103(4)	N2−Cu2−N8	129.58(16)
	Cu2−N6	2.145(4)	N5−Cu2−N6	87.10(15)
	Cu2−N8	1.879(5)		

[a] Numbers in parentheses are the estimated standard deviations of the last significant figure. Atoms are labeled as indicated in Figure 4.

The structure of **2**, shown in Figure 2, features two copper centers that are asymmetrically coordinated by two bdptz ligands and closely resembles that of the related mixed-valent complex, $[Cu_2(bdpdz)_2](ClO_4)_3$, where bdpdz is the pyridazine analogue of bdptz, formed by reduction of a Cu(II) salt.[25,37] The distorted tetrahedral Cu(I) site is ligated by a pair of pyridine groups from each bdptz ligand, whereas the axially elongated pseudo-octahedral environment of the Cu(II) center utilizes the remaining pyridine rings and one phthalazine N donor of each ligand. As a result, one phthalazine nitrogen atom of each bdptz ligand remains unmetalated. A Jahn−Teller distortion accounts for the axial bonds of the Cu(II) site being significantly longer [Cu1−$N_{ax,av}$ = 2.293(2) Å] than the equatorial ones [Cu1−$N_{eq,av}$ = 2.042(1) Å]. The latter are virtually identical to the bond distances of the Cu(I) center [Cu2−N_{av} = 2.055(1) Å]; the anticipated elongation of the metal−ligand bonds upon moving from a coordination number of four to six is offset by the increase in the oxidation state of the copper center, which causes bond contraction. The long Cu···Cu separation of 5.204(2) Å suggests that the unpaired electron is probably not delocalized between the two metal centers.

Examination of **2** by EPR spectroscopy confirms that the valencies are localized. A frozen solution of **2**$(OTf)_3$ in MeOH or MeCN gave a four-line EPR spectrum with $g_{\|}$ = 2.25 ($A_{\|}$ = 169 G) and $g_{\perp}$ = 2.06 at 77 K. This spectrum, shown in Figure 3, is typical of an isolated Cu(II) ion, confirming that **2** is a class I mixed-valent compound,[38] with the unpaired electron localized on the Cu(II) site. A similar spectrum was reported for the closely related pyridazine derivative $[Cu_2(bdpdz)_2](ClO_4)_3$.[25,37] Complex **2** is an example of a synthetic model in which the stereochemistry at the metal centers dictates the location of the unpaired electron.[39] In contrast, the Cu_A centers of cytochrome *c* oxidase and nitrous oxide reductase contain fully delocalized mixed-valent centers in close proximity to each other and display a seven-line EPR spectrum typical for class III mixed-valent dicopper units.[40]

Synthesis and Crystallographic Analysis of Hydroxide-Bridged Dicopper(II) Complexes. Compound **1**$(OTf)_2$ was treated with 1 equiv of AgOTf to determine whether a mixed-valent complex could also be accessed through chemical oxidation. The dicopper(II) complex **3**$(OTf)_3$ was formed, however, indicating that Ag^+ is too strong an oxidant to achieve this goal. As expected, the structure of **3**, shown in Figure 2, is similar to that of the cation in $[Cu_2(bdptz)(\mu\text{-}OH)(H_2O)_2](OTs)_3$, a complex that was prepared directly from $[Cu(H_2O)_6](OTs)_2$.[21] Three coordination sites of each pseudo-square-pyramidal copper(II) ion are occupied by the nitrogen donors of bdptz. In addition to the phthalazine unit, the two Cu(II) centers are also bridged by a single oxygen

(36) Cotton, F. A.; Wilkinson, G. *Advanced Inorganic Chemistry*, 5th ed.; John Wiley & Sons: New York, 1988.
(37) Manzur, J.; García, A. M.; Vega, A.; Spodine, E. *Polyhedron* **1999**, *18*, 2399−2404.
(38) Robin, M. B.; Day, P. In *Advances in Inorganic Chemistry and Radiochemistry*; Emeléus, H. J., Sharpe, A. G., Eds.; Academic Press: New York, 1967; Vol. 10, pp 247−422.
(39) Dunaj-Jurćo, M.; Ondrejović, G.; Melník, M.; Garaj, J. *Coord. Chem. Rev.* **1988**, *83*, 1−28.
(40) Neese, F.; Zumft, W. G.; Antholine, W. E.; Kroneck, P. M. H. *J. Am. Chem. Soc.* **1996**, *118*, 8692−8699.

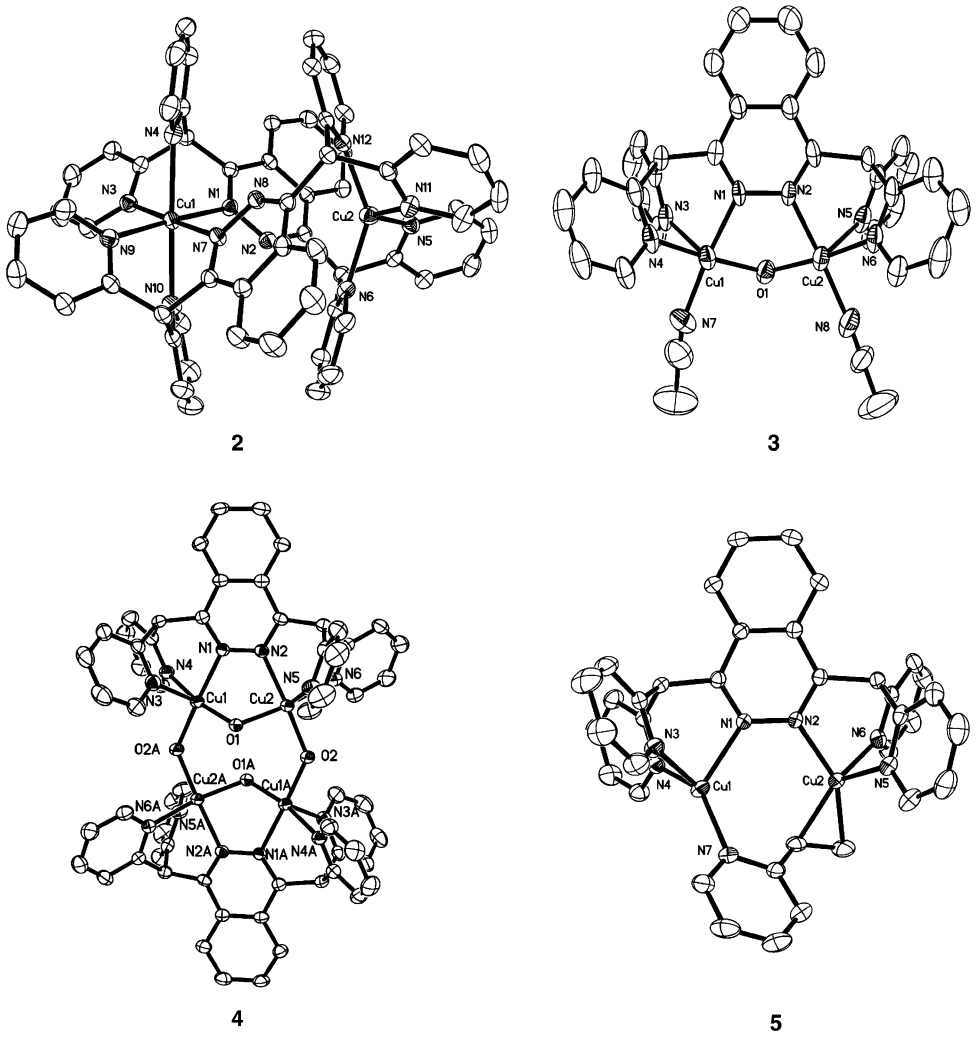

Figure 2. ORTEP diagrams of $[Cu_2(bdptz)_2]^{3+}$ (**2**), $[Cu_2(bdptz)(\mu\text{-OH})(MeCN)_2]^{3+}$ (**3**), $[Cu_2(bdptz)(\mu\text{-OH})_2]_2^{4+}$ (**4**), and $[Cu_2(bdptz)(\mu\text{-vpy})]^{2+}$ (**5**) showing 50% probability thermal ellipsoids for all non-hydrogen atoms (left to right, top to bottom).

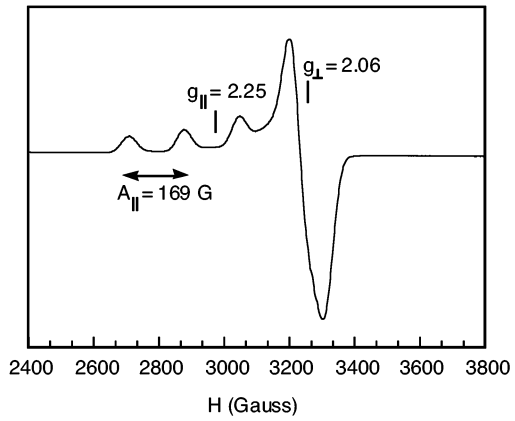

Figure 3. X-band EPR spectrum of **2**$(OTf)_3$ as a frozen solution (4.8 mM in MeOH) at 77 K.

atom. The Cu−O bond distances of 1.909(5) and 1.905(5) Å unequivocally show that this ligand is a hydroxide ion, which was probably introduced as an adventitious solvent component. The Cu−O(H)−Cu bond angle is 112.8(3)°, and the presence of the single-atom bridge significantly diminishes the Cu···Cu separation in **3** to 3.177(1) Å, a reduction of >0.5 Å relative to that in **1**. The Cu−N bond lengths of the pyridine groups bound trans to the hydroxide are substantially shorter [$Cu-N_{av} = 2.004(4)$ Å] than those of the other pyridine ligands [$Cu-N_{av} = 2.282(4)$ Å]. Coordination of an acetonitrile solvent molecule to each metal center completes their coordination spheres.

Reaction of **1**$(OTf)_2$ with dioxygen or treatment of $[Cu(H_2O)_6](OTs)_2$ with bdptz and NaOH in a ratio of 2:1:2 yielded the tetranuclear compound **4**$(OTs)_4$. The structure of cation **4** is composed of two crystallographically equivalent (μ-hydroxo)dicopper(II) units that are joined by two additional hydroxide groups (Figure 2). The $\{Cu_2(bdptz)(\mu\text{-OH})\}^{3+}$ moieties of **4** have bond lengths and angles similar to those in **3**, including the contraction of the Cu−N bond located trans to the bridging hydroxide ligands. The phthalazine-bridged metal ions are separated by 3.169(1) Å with a Cu−O(H)−Cu angle of 112.47(10)°, essentially identical to that found in the structure of **3**. In contrast, the Cu···Cu separation between the two dinuclear units is significantly greater [Cu1···Cu2A = 3.560(1) Å] presumably resulting from the presence of one, rather than two, bridging group and the larger Cu−O(H)−Cu bond angle of 135.19(12)°.

Tetranuclear copper(II) compounds with four hydroxide ligands are known to adopt cubane[41,42] or "stepped-cubane"[43−45] type structures. Prior to this work, the $\{M_4(\mu\text{-}OH)_4\}^{4+}$ structural motif of **4** was not observed with copper(II), although it was characterized with nickel(II),[24] and similar structures of iron(III) with oxo, rather than hydroxo, ligands have also been encountered.[46] The formation of tetranuclear **4**$(OTs)_4$ rather than a bis(μ-hydroxo)-dicopper(II) compound probably results because the geometric restrictions imposed by the bridging phthalazine unit disfavor the $\{Cu_2(\mu\text{-}OH)_2\}^{2+}$ core found in other complexes.[47−50]

Preparation and Crystal Structure of a Bridging Vinylpyridine Dicopper(I) Derivative. Complex **5**$(OTf)_2$ was synthesized in high yield (86%) by the reaction of **1**$(OTf)_2$ with vpy. Both the pyridine N atom and alkene moiety of vpy bind to the dimetallic core. The only other structurally characterized compounds in which vpy coordinates to two metal centers in this fashion are $[Cu_2(\mu\text{-vpy})_2(vpy)_2](ClO_4)_2$[51] and the linear polymers $[(vpy)CuCl]_\infty$ and $[(vpy)CuBr]_\infty$.[52] The η^2 interaction of an alkene[53−61] or aromatic group[62] with copper(I) centers supported by three nitrogen donors is well-documented. It is also noteworthy that copper(I) is the only metal known to bind olefins in nature.[36] In particular, plants utilize a copper(I) center to bind ethylene, a hormone that is involved in many aspects of plant development, including fruit ripening.[63,64]

The structure of cation **5**, shown in Figure 2, reveals that each distorted tetrahedral Cu(I) center is ligated by bdptz in the usual manner, with Cu−N bond distances that average to 2.081(1) Å. The pyridine N atom of the vpy ligand coordinates to Cu1 with a bond length of 1.951(2) Å, which is somewhat shorter than the corresponding bonds in the complex $[Cu_2(\mu\text{-vpy})_2(vpy)_2](ClO_4)_2$ (1.981(9) and 2.008(10) Å).[51] Coordination of the alkene moiety to Cu2 is asymmetric, as was observed in $[Cu_2(\mu\text{-vpy})_2(vpy)_2](ClO_4)_2$, with longer bond lengths for the inner (2.050(3) Å) than the outer (2.008(3) Å) olefinic carbon atoms. The olefinic C═C bond length in **5** of 1.368(4) Å matches well with those of the coordinated vpy ligands in $[Cu_2(\mu\text{-vpy})_2(vpy)_2](ClO_4)_2$ (1.358(16) and 1.368(17) Å) and is slightly longer than those of the noncoordinated vpy C═C groups (1.319(23) and 1.307(23) Å) in the latter complex.

Synthesis and Structural Characterization of a Bis-(acetonitrile) Complex with Ph_4bdptz. Tetranuclear compounds such as **4**$(OTs)_4$ form through undesired bimolecular interactions, frequently resulting from oxidation reactions. Because bdptz supports such structures with several first-row transition-metal ions, we introduced the sterically hindered derivative Ph_4bdptz in an effort to prevent the formation of the high-nuclearity species. Treatment of $[Cu(MeCN)_4](OTf)$ with Ph_4bdptz in a 2:1 ratio afforded **6**$(OTf)_2$ in >70% yield. As an analogue of **1**, compound **6** also serves as a useful starting material. Although the triflate salt is a flocculent solid, single crystals suitable for X-ray crystallographic study were obtained when BF_4^- was used as the counterion.

The geometry around the copper centers in cation **6**, shown in Figure 4, is similar to that in **1**. The copper(I) ions are separated by 3.792(1) Å, which is ∼0.05 Å longer than the Cu···Cu distance in **1**. The average Cu−N(Ph_4bdptz) bond length of 2.115(2) Å is substantially longer than the Cu−N(MeCN) bond distances of 1.893(4) and 1.879(5) Å. This difference in bond lengths is evident in related compounds containing $\{N_3(aromatic)Cu^I(MeCN)\}$ fragments[65−67] and is a result of the different nitrogen-atom orbital hybridizations and lesser steric demands of the linear CH_3CN ligand. The Cu−N bond lengths in **6** are slightly longer than the corresponding distances in **1** ($\Delta_{Cu-N(bdptz')} \sim 0.05$, $\Delta_{Cu-N(MeCN)} \sim 0.02$ Å). The increased metal−ligand and metal−metal distances in **6** relative to the bdptz analogue result from a combination of electronic and steric factors; the electron-withdrawing phenyl rings of Ph_4bdptz weaken the Cu−N bonds, and the steric repulsion created by the proximity of these bulky groups is minimized when the ligand components are farther from the metal centers. The N(Ph_4bdptz)−Cu−N(Ph_4bdptz) bond angles average out to ∼90°, and the N(Ph_4bdptz)−Cu−N(MeCN) bond angles

(41) Sletten, J.; Sørensen, A.; Julve, M.; Journaux, Y. *Inorg. Chem.* **1990**, *29*, 5054−5058.
(42) Dedert, P. L.; Sorrell, T.; Marks, T. J.; Ibers, J. A. *Inorg. Chem.* **1982**, *21*, 3506−3517.
(43) van Albada, G. A.; Mutikainen, I.; Roubeau, O.; Turpeinen, U.; Reedijk, J. *Inorg. Chim. Acta* **2002**, *331*, 208−215.
(44) Zheng, Y.-Q.; Lin, J.-L. *Z. Anorg. Allg. Chem.* **2002**, *628*, 203−208.
(45) Mathews, I. I.; Manohar, H. *J. Chem. Soc., Dalton Trans.* **1991**, 2139−2143.
(46) Barrios, A. M.; Lippard, S. J. Unpublished results.
(47) van Albada, G. A.; Mutikainen, I.; Turpeinen, U.; Reedijk, J. *Inorg. Chim. Acta* **2001**, *324*, 273−277.
(48) Youngme, S.; Somjitsripunya, W.; Chinnakali, K.; Chantrapromma, S.; Fun, H.-K. *Polyhedron* **1999**, *18*, 857−862.
(49) Mann, K. L. V.; Jeffery, J. C.; McCleverty, J. A.; Thornton, P.; Ward, M. D. *J. Chem. Soc., Dalton Trans.* **1998**, 89−97.
(50) Wu, L.-P.; Keniry, M. E.; Hathaway, B. *Acta Crystallogr., Sect. C* **1992**, *48*, 35−40.
(51) Munakata, M.; Kitagawa, S.; Simono, H.; Emori, T.; Masuda, H. *J. Chem. Soc., Chem. Commun.* **1987**, 1798−1799.
(52) Engelhardt, L. M.; Healy, P. C.; Kildea, J. D.; White, A. H. *Aust. J. Chem.* **1989**, *42*, 185−199.
(53) Dias, H. V. R.; Lu, H.-L.; Kim, H.-J.; Polach, S. A.; Goh, T. K. H. H.; Browning, R. G.; Lovely, C. J. *Organometallics* **2002**, *21*, 1466−1473.
(54) Zhang, J.; Xiong, R.-G.; Zuo, J.-L.; Che, C.-M.; You, X.-Z. *J. Chem. Soc., Dalton Trans.* **2000**, 2898−2900.
(55) Shimazaki, Y.; Yokoyama, H.; Yamauchi, O. *Angew. Chem., Int. Ed.* **1999**, *38*, 2401−2403.
(56) Sanyal, I.; Murthy, N. N.; Karlin, K. D. *Inorg. Chem.* **1993**, *32*, 5330−5337.
(57) Nelson, S. M.; Lavery, A.; Drew, M. G. B. *J. Chem. Soc., Dalton Trans.* **1986**, 911−920.
(58) Thompson, J. S.; Harlow, R. L.; Whitney, J. F. *J. Am. Chem. Soc.* **1983**, *105*, 3522−3527.
(59) Pasquali, M.; Floriani, C.; Gaetani-Manfredotti, A.; Chiesi-Villa, A. *Inorg. Chem.* **1979**, *18*, 3535−3542.
(60) Pasquali, M.; Floriani, C.; Gaetani-Manfredotti, A.; Chiesi-Villa, A. *J. Am. Chem. Soc.* **1978**, *100*, 4918−4919.
(61) Dai, X.; Warren, T. H. *Chem. Commun.* **2001**, 1998−1999.
(62) Osako, T.; Tachi, Y.; Taki, M.; Fukuzumi, S.; Itoh, S. *Inorg. Chem.* **2001**, *40*, 6604−6609.
(63) Rodríguez, F. I.; Esch, J. J.; Hall, A. E.; Binder, B. M.; Schaller, G. E.; Bleecker, A. B. *Science* **1999**, *283*, 996−998.
(64) Dey, P. M., Harborne, J. B., Eds. *Plant Biochemistry*; Academic Press: London, 1997.
(65) Jonas, R. T.; Stack, T. D. P. *Inorg. Chem.* **1998**, *37*, 6615−6629.
(66) Blake, A. J.; Hill, S. J.; Hubberstey, P.; Li, W.-S. *J. Chem. Soc., Dalton Trans.* **1998**, 909−915.
(67) Canty, A. J.; Engelhardt, L. M.; Healy, P. C.; Kildea, J. D.; Minchin, N. J.; White, A. H. *Aust. J. Chem.* **1987**, *40*, 1881−1891.

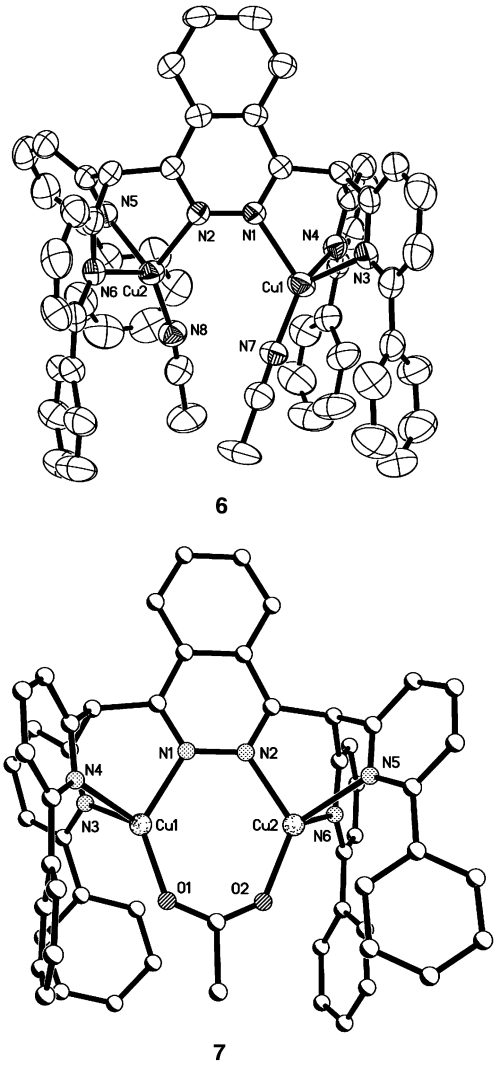

Figure 4. ORTEP diagram of $[Cu_2(Ph_4bdptz)(MeCN)_2]^{2+}$ (**6**) showing 50% probability thermal ellipsoids for all non-hydrogen atoms and a ball-and-stick representation of $[Cu_2(Ph_4bdptz)(\mu\text{-}O_2CCH_3)]^+$ (**7**) (top to bottom).

range from 113.63(16) to 140.39(17)°, similar to the angles found in the C_s- and C_{3v}-symmetric mononuclear copper(I) compounds with facial-capping N-donor ligands.[65,68,69] These bond angles are essentially unchanged relative to those in **1**.

Preparation of a Carboxylate-Bridged Dicopper(I) Complex. In contrast to the mixed-valent compound **2**$(OTf)_3$, which was isolated using the bdptz analogue, reaction of **6**$(OTf)_2$ with NaO_2CCH_3 yields the acetate-bridged dicopper(I) complex **7**(OTf). The steric bulk provided by the phenyl substituents of Ph_4bdptz precludes the formation of a compound with a structure similar to that of **2**, and the high redox potentials of **6** (vide infra) stabilize the +1 oxidation state and disfavor disproportionation. The synthesis of **7**(OTf) proceeds in a mixture of CH_2Cl_2 and MeOH. The latter solvent is necessary to dissolve NaO_2CCH_3, and no reaction occurs in its absence, even after prolonged reaction times (>12 h) did not improve matters. Furthermore, the reaction does not go to completion even in the presence of a large excess of NaO_2CCH_3 (>20 equiv), as evidenced by the isolation of a mixture of **6**$(OTf)_2$ and **7**(OTf). This result is probably due to MeCN being a better ligand than acetate for copper(I) and is supported by the complete regeneration of **6**$(OTf)_2$ from the mixture upon addition of MeCN.

A full crystallographic refinement of **7**(OTf) was hampered by the severe disorder of the triflate counterion, and the substitution of triflate by BF_4^-, PF_6^-, ClO_4^-, or BPh_4^- did not afford single crystals of suitable quality to permit analysis by X-ray diffraction. The structure of cation **7** is shown in Figure 4. Briefly, Ph_4bdptz coordinates two copper(I) ions in the usual manner, and the acetate ligand bridges the metal centers with Cu−O bond distances of ∼1.93 Å. The Cu···Cu separation of ∼3.53 Å is shorter than that in **1** and **6**, which lack a second bridging ligand, but longer than in the single-atom-bridged cations **3** and **4**. Whereas (μ-carboxylato)dicopper(II) compounds are common, the analogous dicopper(I) complexes are rare, typically requiring π-acceptor ancillary ligands,[70−73] sterically demanding and preorganized bis(carboxylate) platforms,[74,75] or a copper−copper interaction.[76]

Electrochemical Studies of Compounds 1$(OTf)_2$ and 2$(OTf)_3$. Cyclic voltammograms (CVs) of compounds **1**$(OTf)_2$, **2**$(OTf)_3$, and **6**$(OTf)_2$ were recorded in MeCN, and the $E_{1/2}$ values of **2**$(OTf)_3$, **6**$(OTf)_2$, and selected mononuclear and dinuclear compounds are compiled in Table 5. Compound **1** showed highly irreversible electrochemical behavior, indicating that the dinuclear core is not stable under these conditions. Compound **2**, on the other hand, displayed a reversible wave with an $E_{1/2}$ value of −452 mV (ΔE_p = 74 mV) versus Cp_2Fe^+/Cp_2Fe when potentials lower than −100 mV were applied. Application of higher potentials resulted in irreversible redox waves, as shown in Figure 5. When converted to the same scale, the $Cu^{II}Cu^{II}/Cu^{II}Cu^{I}$ couple of **2** is more than 150 mV below that of $[Cu_2(bdpdz)_2](ClO_4)_3$.[25,37] Although the two compounds are structurally very similar, phthalazine (pK_a = 3.47)[77] is a stronger base than pyridazine (pK_a = 2.24),[77] which may explain why the copper(I) center in **2** is easier to oxidize. The redox potential of **2** is comparable to that of the copper(I) complexes [Cu(TMPA)(MeCN)](ClO_4),[25,78,79] [Cu(H-MePY2)]$(B(C_6H_5)_4)$,[25,80] and $[Cu_2(bTMPA)](ClO_4)_2$,[25,81] all of which bear ligands featuring a combination of pyridine and amine substituents.

(68) Lam, B. M. T.; Halfen, J. A.; Young, V. G., Jr.; Hagadorn, J. R.; Holland, P. L.; Lledós, A.; Cucurull-Sánchez, L.; Novoa, J. J.; Alvarez, S.; Tolman, W. B. *Inorg. Chem.* **2000**, *39*, 4059−4072.
(69) Conry, R. R.; Ji, G.; Tipton, A. A. *Inorg. Chem.* **1999**, *38*, 906−913.
(70) Kitagawa, S.; Kondo, M.; Kawata, S.; Wada, S.; Maekawa, M.; Munakata, M. *Inorg. Chem.* **1995**, *34*, 1455−1465.
(71) Toth, A.; Floriani, C.; Chiesi-Villa, A.; Guastini, C. *Inorg. Chem.* **1987**, *26*, 236−241.
(72) Pasquali, M.; Floriani, C.; Venturi, G.; Gaetani-Manfredotti, A.; Chiesi-Villa, A. *J. Am. Chem. Soc.* **1982**, *104*, 4092−4099.
(73) Pasquali, M.; Leoni, P.; Floriani, C.; Gaetani-Manfredotti, A. *Inorg. Chem.* **1982**, *21*, 4324−4328.
(74) Hagadorn, J. R.; Zahn, T. I.; Que, L., Jr.; Tolman, W. B. *Dalton Trans.* **2003**, 1790−1794.
(75) LeCloux, D. D.; Lippard, S. J. *Inorg. Chem.* **1997**, *36*, 4035−4046.
(76) He, C.; Lippard, S. J. *Inorg. Chem.* **2000**, *39*, 5225−5231.
(77) Gilchrist, T. L. *Heterocyclic Chemistry*, 3rd ed.; Addison-Wesley Longman Ltd.: Essex, U.K., 1997.
(78) Zhang, C. X.; Kaderli, S.; Costas, M.; Kim, E.; Neuhold, Y.-M.; Karlin, K. D.; Zuberbühler, A. D. *Inorg. Chem.* **2003**, *42*, 1807−1824.
(79) Lee, D.-H.; Wei, N.; Murthy, N. N.; Tyeklár, Z.; Karlin, K. D.; Kaderli, S.; Jung, B.; Zuberhüler, A. D. *J. Am. Chem. Soc.* **1995**, *117*, 12498−12513.

Table 5. CV Data for Compounds **2**$(OTf)_3$, **6**$(OTf)_2$, and Related Mononuclear and Dinuclear Models

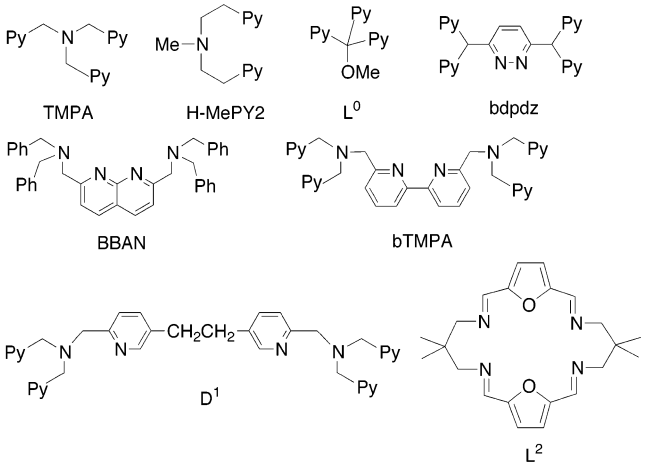

complex	$E_{1/2}$[a]	solvent	ref
$[Cu(TMPA)(MeCN)](ClO_4)$	−400	MeCN	78
	−628[b]	DMF	79
$[Cu(H\text{-}MePY2)](B(C_6F_5)_4)$	−310	DMF	80
$[Cu(L^0)(MeCN)](OTf)$	+60[c]	$MeCN/CH_2Cl_2$	65
$[Cu_2(bdpdz)_2](ClO_4)_3$	−290[d]	$MeCN/H_2O$	37
$[Cu_2(BBAN)(\mu\text{-}O_2CCPh_3)](OTf)$	−25	THF	76
$[Cu_2(bTMPA)](ClO_4)_2$	−346[e]	DMF	81
$[Cu_2(D^1)(MeCN)_2](ClO_4)_2$	−639[b]	DMF	79
$[Cu_2(L^2)(MeCN)_2](ClO_4)_2$	+140[f]	MeCN	83
	+568[f]		
2	−452	MeCN	this paper
6	+41	MeCN	this paper
	+516		

[a] mV(vs Cp_2Fe^+/Cp_2Fe). [b] $Cp_2Fe^+/Cp_2Fe = +20$ mV versus $Ag/AgNO_3$. [c] $Cp_2Fe^+/Cp_2Fe = +450$ mV versus saturated calomel electrode (SCE). [d] $Cp_2Fe^+/Cp_2Fe = +380$ mV versus SCE in MeCN with $(Bu_4N)ClO_4$ as the supporting electrolyte (see: Connelly, N. G.; Geiger, W. E. *Chem. Rev.* **1996**, *96*, 877−910). [e] $Cp_2Fe^+/Cp_2Fe = +545$ mV versus Ag/AgCl. [f] $Cp_2Fe^+/Cp_2Fe = +401$ mV versus Ag/AgCl.

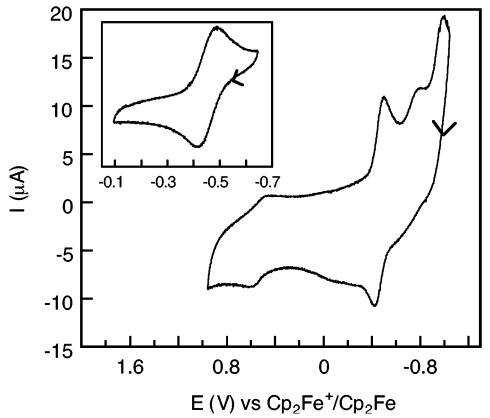

Figure 5. CVs of 2 mM **2**$(OTf)_3$ in MeCN with 0.5 M $Bu_4N(PF_6)$ as the supporting electrolyte. The full CV was recorded with a scan rate of 200 mV/s, and the inset shows the CV recorded with a scan rate of 100 mV/s when potentials below −0.1 V versus Cp_2Fe^+/Cp_2Fe were applied.

In contrast, the $E_{1/2}$ value of **2** is significantly more negative than that of $[Cu(L^0)(MeCN)](OTf)$, the +1 oxidation state

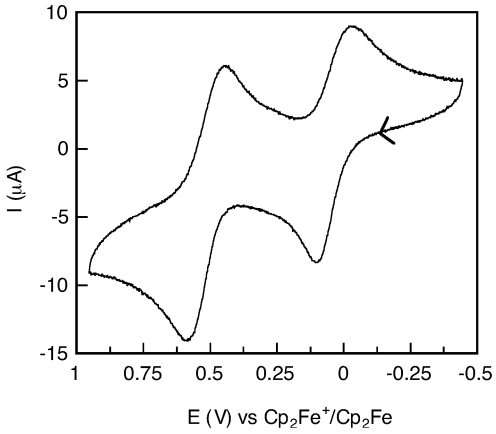

Figure 6. CV of 2 mM **6**$(OTf)_2$ in MeCN with 0.5 M $Bu_4N(PF_6)$ as the supporting electrolyte and a scan rate of 100 mV/s.

of which is stabilized by the facially capping tris(pyridyl) moiety.[25,65]

Electrochemistry of 6(OTf)$_2$. Irreversible electrochemical behavior was observed with **6** in CH_2Cl_2. In contrast, two well-separated reversible waves with $E_{1/2}$ potentials of +41 mV ($\Delta E_p = 122$ mV) and +516 mV ($\Delta E_p = 124$ mV) versus Cp_2Fe^+/Cp_2Fe corresponding to the $Cu^{II}Cu^I/Cu^ICu^I$ and Cu^{II}-$Cu^{II}/Cu^{II}Cu^I$ couples, respectively, were observed when MeCN was employed as the solvent (Figure 6). Evidently, the species generated electrochemically from **6** are stabilized in the coordinating solvent. Addition of MeCN often improves the reversibility of CV traces of copper(I) compounds, possibly by providing an additional ligand to stabilize the copper(II) species.[65,82] The relatively high redox potentials displayed by **6** compared to the majority of the compounds listed in Table 5 are probably largely due to the electron-withdrawing phenyl substituents of Ph_4bdptz, which make oxidation to Cu(II) more difficult. Electrochemical studies on a series of dicopper(I) complexes supported by macrocyclic ligands, including the compound $[Cu_2(L^2)$-$(MeCN)_2](ClO_4)_2$, also showed well-resolved sequential one-electron redox waves at comparably high potentials.[25,83] By using the $E_{1/2}$ values for the two redox couples, a comproportionation constant, K_{com}, of 1×10^8 was calculated for **6** according to the equilibrium in eq 2.[84] The large value of

$$[Cu^ICu^I(Ph_4bdptz)]^{2+} + [Cu^{II}Cu^{II}(Ph_4bdptz)]^{4+} \overset{K_{com}}{\rightleftharpoons} 2[Cu^ICu^{II}(Ph_4bdptz)]^{3+} \quad (2)$$

K_{com}, comparable to that determined for $[Cu_2(L^2)(MeCN)_2]$-$(ClO_4)_2$ ($K_{com} = 2 \times 10^7$),[25,83] suggests that the mixed-valent species should have significant thermodynamic stability, although attempts to generate it from **6** have thus far been unsuccessful. In contrast to the two redox waves seen with **6**, only one apparent wave, corresponding to the oxidation

(80) Zhang, C. X.; Liang, H.-C.; Kim, E.; Shearer, J.; Helton, M. E.; Kim, E.; Kaderli, S.; Incarvito, C. D.; Zuberbühler, A. D.; Rheingold, A. L.; Karlin, K. D. *J. Am. Chem. Soc.* **2003**, *125*, 634−635.
(81) Lee, D.-H.; Murthy, N. N.; Karlin, K. D. *Inorg. Chem.* **1997**, *36*, 5785−5792.
(82) Carrier, S. M.; Ruggiero, C. E.; Houser, R. P.; Tolman, W. B. *Inorg. Chem.* **1993**, *32*, 4889−4899.
(83) Yates, P. C.; Drew, M. G. B.; Trocha-Grimshaw, J.; McKillop, K. P.; Nelson, S. M.; Ndifon, P. T.; McAuliffe, C. A.; Nelson, J. *J. Chem. Soc., Dalton Trans.* **1991**, 1973−1979.
(84) Gagné, R. R.; Koval, C. A.; Smith, T. J.; Cimolino, M. C. *J. Am. Chem. Soc.* **1979**, *101*, 4571−4580.

of both copper centers, is displayed by $[Cu_2(bTMPA)](ClO_4)_2$ and $[Cu_2(D^1)(MeCN)_2](ClO_4)_2$. This result indicates that the two noninteracting metal ions in each of these latter compounds are oxidized at approximately the same potential.[25,79,81] The bridging phthalazine unit in **6**, therefore, confers greater communication between the copper ions.

Dioxygen Reactivity Studies of Dicopper Complexes. The addition of dioxygen to an orange solution of **1**$(OTf)_2$ in MeOH at −78 °C caused an immediate color change to pale green. Similar behavior was observed when low-temperature oxygenations were performed in CH_2Cl_2 or MeCN. The optical spectrum of the reaction products does not indicate the formation of a copper−dioxygen adduct such as a peroxo, bis(μ-oxo), or superoxo intermediate, all of which have distinctive electronic transitions in the visible region.[85] Oxygenation of **1** afforded the tetranuclear compound **4**, possibly by dimerization of a (peroxo)dicopper(II) species followed by rearrangement.[86] If a $\{Cu_2O_2\}^{2+}$ adduct were generated in the initial stages of the reaction, it might form and decay too rapidly to allow observation by either conventional UV−vis spectroscopy or stopped-flow methods at −60 °C. Reaction of dioxygen with a solution of mixed-valent **2** in CH_2Cl_2 proceeded more slowly, turning the solution green only after several hours at room temperature. This decreased reactivity is inconsistent with the low redox potential of the compound and may result from restricted access of dioxygen to the copper(I) site. Although the final product has not been characterized, oxidation of the pyridazine analogue afforded a mixture of $[Cu_2(bdpdz)_2](ClO_4)_4$ and a compound formulated as $[Cu_2(bdpdz)_2(OH)_2](ClO_4)_2$.[25,37] Oxygenation of **5** in CH_2Cl_2, MeOH, or MeCN proceeded similarly to that of **1** and also afforded the tetranuclear species. No activation of the vinyl substituent of **5** was detected in either the presence or absence of the proton source $[H(OEt_2)_2](BAr'_4)$[25,87] or when H_2O_2 was used as an oxidant. Related compounds similarly oxidized to Cu(II) without involvement of an alkene unit.[56,61]

The sterically hindered Ph_4bdptz ligand was expected to prevent the formation of tetranuclear species because of the presence of the phenyl rings on the pyridine groups that extend well below the line joining the two copper centers. An attractive feature of Ph_4bdptz is that the phenyl groups form a hydrophobic cavity in which the two copper centers are positioned in such a way as to provide a binding pocket. This property has potential value for the activation of small-molecule substrates in future work. The steric bulk provided by the pocket, however, appears to affect the access of O_2 to the dimetallic core and significantly diminishes the reactivity of compounds supported by this ligand. The decreased reactivity toward dioxygen is consistent with the rather high redox potentials of **6** observed by CV. Compound **6** is inert to dioxygen in MeCN but turns brown over several minutes upon exposure to dioxygen in CH_2Cl_2. Similarly, addition of H_2O_2 to a solution of **6** in MeCN afforded a brown solution at room temperature, but no reaction occurred at −40 °C. The decreased dioxygen reactivity of Ph_4bdptz relative to the bdptz complexes is also shared by complex **7**, which is an air-stable solid that turns green in solution only after several weeks at room temperature. Attempts to crystallize the product of the reaction between **6** and dioxygen have thus far been unsuccessful. Analysis of the reaction mixture by ESI-MS (see the Supporting Information, Figures S1−S3) shows peaks corresponding to a number of different compounds including unreacted **6** and mononuclear copper(I) compounds. A peak at $m/z = 1062$, however, exhibits the correct mass and isotope pattern for $\{[Cu_2(Ph_4\text{-bdptz})](OTf)\}^+$ after the loss of a proton and incorporation of an oxygen atom, possibly corresponding to the hydroxylation of a phenyl ring of the Ph_4bdptz ligand. Aromatic hydroxylation by copper(I) complexes upon reaction with dioxygen is well-precedented,[9,11,14] and charge balance could be attained by a mixed-valent Cu(I)Cu(II) species such as that shown in Figure S3 of the Supporting Information.

Conclusions

A family of dicopper compounds were prepared and characterized with the ligands bdptz and Ph_4bdptz. The phthalazine bridge supports a range of metal···metal distances and a variety of ancillary ligands but does not permit the detection of dioxygen adducts. The incorporation of the phenyl substituents in Ph_4bdptz prevents the formation of undesired high-nuclearity species, however, and allows the observation of two reversible redox waves by CV.

A difficult feature of metalloenzymes to model effectively is the composition and chemistry of their secondary coordination spheres. Many proteins have a hydrophobic channel that facilitates access of small molecules to the active site, which is buried in the protein interior. The phenyl rings of Ph_4bdptz form a binding pocket that mirrors this property and suggests a general strategy for the introduction of secondary sphere components into a dinucleating scaffold.

Acknowledgment. This work was supported by grants from the National Science Foundation and National Institute of General Medical Sciences. J.K. acknowledges NSERC for a graduate student fellowship. We thank Ms. Li Li of the MIT Department of Chemistry Instrumentation Facility for performing the ESI-MS measurements and Professor Thomas J. Smith for valuable discussions.

Supporting Information Available: ESI-MS spectra of oxidized solutions of **6**$(OTf)_2$, the full numbering schemes of **2**−**6**, scan rate plots for **2**$(OTf)_3$ and **6**$(OTf)_2$, and X-ray crystallographic files in CIF format. This material is available free of charge via the Internet at http://pubs.acs.org.

IC035009R

(85) Blackman, A. G.; Tolman, W. B. *Struct. Bonding* **2000**, *97*, 179−211.
(86) Feig, A. L.; Becker, M.; Schindler, S.; van Eldik, R.; Lippard, S. J. *Inorg. Chem.* **1996**, *35*, 2590−2601.
(87) Brookhart, M.; Grant, B.; Volpe, A. F., Jr. *Organometallics* **1992**, *11*, 3920−3922.